NUCLEAR SCIENCE AND TECHNIQUES **26**, S20503 (2015)

# A nuclear density probe: isobaric yield ratio difference*

YU Mian (于勉),[1,2] DUAN Kun-Jie (段坤杰),[3] Wang Shan-Shan (王闪闪),[2,4]
ZHANG Yan-Li (张艳丽),[2] and Ma Chun-Wang (马春旺)[2,†]

[1]*Xinxiang Medical University, Xinxiang 453003, China*
[2]*Institute of Particle and Nuclear Physics, Henan Normal University, Xinxiang 453007, China*
[3]*Henan University of Urban Construction, Pingdingshan 467036, China*
[4]*Shanghai Institute of Applied Physics, Chinese Academy of Sciences, Shanghai 201800, China*
(Received January 2, 2015; accepted in revised form January 26, 2015; published online April 20, 2015)

We report our recent progress on the nuclear symmetry energy probe, which is called the isobaric yield ratio difference (IBD), and its application in neutron density determination in experiments. The results obtained by the IBD, from which the isobaric yields in the measured $140A$ MeV $^{40,48}$Ca + $^{9}$Be and $^{58,64}$Ni + $^{9}$Be reactions, and the calculated $80A$ MeV $^{38\text{-}52}$Ca + $^{12}$C reactions by using a modified statistical abrasion-ablation model, show the sensitivity of the IBD to the density differences between reactions.

Keywords: Isobaric yield ratio difference, Symmetry energy, Neutron density, Neutron-rich nucleus

DOI: 10.13538/j.1001-8042/nst.26.S20503



## I. INTRODUCTION

The symmetry energy of asymmetric nuclear matter, especially neutron-rich matter, has been an important topic in both theory and experiment with the development of radioactive nuclear beam (RNB) facilities. The new or updated RNB facilities can provide nuclear beams with larger neutron-richness, which are supposed to promote the study of neutron-rich nuclear matter and extend the chart of nuclides to the more neutron-rich side. In heavy-ion collisions above the intermediate energy, nuclear matter from sub-saturation to supra-saturation densities can be produced. The symmetry energy of nuclear matter depends on density and temperature. In the past decade, though many probes have been proposed, there are still difficulties in measuring the symmetry energy of nuclear matter at different nuclear densities.

The isobaric yield ratio (IYR) method was first proposed by Huang *et al.* to extract the symmetry-energy coefficient for fragments with small isospins, which also have some temperature since they are measured in heavy-ion collision [1, 2]. In the IYR, some terms deciding the fragment yield cancel out, which makes it useful to study the symmetry energy term of the fragment with a low temperature. The IYR method is extended to study the symmetry energy of fragment with larger neutron richness [3–6]. The results obtained by the IYR method are compared to a similar method, i.e., isoscaling, which extracts the symmetry energy of the colliding source, showing a large difference between them [7–10]. We studied the results of the IYR and isoscaling, and found that though the IYR and isoscaling methods both aim at the extraction of nuclear symmetry energy, the obtained results are for different nuclear matter. A new probe was constructed via IYR between two reactions, which is called the isobaric yield ratio difference (IBD), and the results of the IBD and isoscaling were found to be similar because they are both the probes for the chemical potential of neutrons and protons in the reactions [11, 12]. Moreover, the IBD probe is also sensitive to the density differences between the reactions [13, 14]. In this article, we will summarize the recent progress on the IBD method.

## II. THEORETICAL DESCRIPTIONS

In thermodynamics theory, an equilibrium state is assumed for the reaction, which introduces the concept of temperature. The temperature affects the yield of fragment. With high temperature, light particles like neutrons and protons can escape from the binding of hot fragment. The formation time of the final fragments, which correspond to the measured ones in experiments, is called the "chemical freeze-out" (when the fragment ceases to emit light particles, like neutrons, protons or $\alpha$, and the neutron and proton numbers do not change anymore). In general, the yield of fragment in heavy-ion collisions above the Fermi energy obeys an exponential law. For example, in the grand-canonical ensembles theory within the grand canonical limit, the yield of a fragment with mass numbers $A$ and neutron-excess $I$ ($I = N–Z$ is the difference between the numbers of neutrons and protons) is written as [15, 16]

$$\sigma(I,A) = cA^{\tau}\exp\{[F(I,A) + N\mu_n + Z\mu_p]/T\}, \quad (1)$$

where $T$ is the temperature of the system. $F(I,A)$ is the free energy of the fragment which depends on $T$. $\mu_n(\mu_p)$ is the chemical potential of the neutrons (protons) in the equilibrium system, which depends on the density and $T$ of the systems. In the isoscaling method [17, 18], the difference between the $\mu_n(\mu_p)$ of two reactions can be extracted from the isotopic (isotonic) ratio

$$R(I,A)_{21} = \frac{\sigma(I,A)_2}{\sigma(I,A)_1} \propto \exp\{[N(\mu_{n2}-\mu_{n1}) + Z(\mu_{p2}-\mu_{p1})]/T\}, \quad (2)$$

* Supported by the Program for Science & Technology Innovation Talents in Universities of Henan Province (No. 13HASTIT046) and the Young Teacher Project in Henan Normal University
† Corresponding author, machunwang@126.com

with indices 1 and 2 denoting the reactions. In Eq. (2), the $T$ of the two reactions is assumed to be the same. For the chemical freeze-out fragments this can be true since they both have a very long evolution time. For the isotopic ratio,

$$\ln R(I,A)_{21} = [N(\mu_{n2}-\mu_{n1}) + Z(\mu_{p2}-\mu_{p1})]/T, \quad (3)$$

$Z$ does not change. The isotopic ratio shows scaling phenomena obeying the linear function. The fitted slope is defined as $\alpha \equiv (\mu_{n2}-\mu_{n1})/T$. Similarly, for the isotonic ratio, $N$ is a constant. The isotonic ratio also shows scaling phenomena obeying the linear function. The fitted slope is defined as $\beta \equiv (\mu_{p2}-\mu_{p1})/T$. $\alpha$ and $\beta$ are used to extract the symmetry energy of the system. But the symmetry energy in the isoscaling method is an indirect result obtained from the yield of fragments.

Starting from Eq. (1), assuming the isobars differing 2 units in $I$ have the same temperature, the isobaric yield ratio can be defined as

$$\begin{aligned} R(I+2,I,A)_{21} &= \frac{\sigma(I+2,A)}{\sigma(I,A)} \\ &= \exp\{[F(I+2,A) - F(I,A) + \mu_n - \mu_p]/T\}. \end{aligned} \quad (4)$$

To make cancellation of $F$, we adopt a reference reaction system with similar measurements as the isoscaling method does, and assume that the free energies of one fragment in the two reactions are the same. Defined as the difference between the IYRs of two reactions, the IBD is [11, 12]

$$\begin{aligned} \Delta\ln R(I+2,I,A)_{21} &= \ln R_2(I+2,I,A) - \ln R_1(I+2,I,A) \\ &= [(\mu_{n2}-\mu_{n1}) - (\mu_{p2}-\mu_{p1})]/T \\ &= (\Delta\mu_{n21} - \Delta\mu_{p21})/T = \Delta\mu_{21}/T. \end{aligned} \quad (5)$$

The indices also denote the reaction systems. From the definition of the isoscaling parameters, the following correlation can be obtained

$$\Delta\ln R(I+2,I,A)_{21} = \alpha - \beta. \quad (6)$$

Eq. (5) can also be written as

$$\begin{aligned} \Delta\ln R(I+2,I,A)_{21} &= [(\mu_{n2}-\mu_{p1}) - (\mu_{n1}-\mu_{p1})]/T \\ &= (\Delta\mu_{np2} - \Delta\mu_{np1})/T. \end{aligned} \quad (7)$$

The chemical potentials of neutrons and protons are related to the densities of neutrons ($\rho_n$) and protons ($\rho_p$) respectively [14, 19]

$$\mu_n/T = \ln\rho_n, \quad \text{and} \quad \mu_p/T = \ln\rho_p, \quad (8)$$

which result in $\alpha = \ln\rho_{n2} - \ln\rho_{n1} = \ln(\rho_{n2}/\rho_{n1})$, and $\beta = \ln\rho_{p2} - \ln\rho_{p1} = \ln(\rho_{p2}/\rho_{p1})$. We can also write the relationship between the IBD results and the densities of the reaction systems as [14]

$$\Delta\ln R(I+2,I,A)_{21} = \ln(\rho_{n2}/\rho_{n1}) - \ln(\rho_{p2}/\rho_{p1}), \quad (9)$$

$$\Delta\ln R(I+2,I,A)_{21} = \ln(\rho_{n2}/\rho_{p2}) - \ln(\rho_{n1}/\rho_{p1}). \quad (10)$$

Eqs. (9) and (10) are written according to Eqs. (5) and (7), respectively. The densities of protons can be determined by experimental measurement. Thus the relationships in Eqs. (9) and (10) can be used to determine the neutron density of the neutron-rich system. For example, if the reference reaction system is a neutron-proton symmetric one, in which $\rho_{n1}$ and $\rho_{p1}$ can be assumed to be the same and $\rho_{p2}$ is measurable, $\rho_{n2}$ can be determined from the IBD results. In Eq. (9), if $\rho_{p2}$ and $\rho_{p1}$ can be assumed to be the same (for isotopic projectiles) and $\rho_{p1} \approx \rho_{n1}$, $\Delta R(I+2,I,A)_{21} = \ln(\rho_{n2}/\rho_{p1})$. Similarly, in Eq. (10), the reference reaction is neutron-proton symmetric and $\rho_{p1} \approx \rho_{n1}$, by knowing $\rho_{p2}$, $\Delta R(I+2,I,A)_{21} = \ln(\rho_{n2}/\rho_{p2})$ and $\rho_{n2}$ can be determined from the IBD.

## III. RESULTS AND DISCUSSION

We will show the IBD results obtained from the measured 140$A$ MeV $^{40,48}$Ca + $^{9}$Be and $^{58,64}$Ni + $^{9}$Be projectile fragmentation reactions [20]. These reactions were measured by M. Mocko *et al.* at the National Superconducting Cyclotron Laboratory (NSCL) at Michigan State University. The measured fragments range from $Z = 5$ to $Z_{\rm proj}$, which provides high quality data for the test of the IBD methods. The IBD results has been previously reported [11].

In Fig. 1, the results of the IBD and isoscaling methods are re-plotted for comparison [11]. Four groups of reactions are analyzed, the $^{48}$Ca/$^{40}$Ca + $^{9}$Be and $^{64}$Ni/$^{58}$Ni + $^{9}$Be reactions of the isotopic projectiles, the $^{58}$Ni/$^{40}$Ca + $^{9}$Be reactions with the projectiles both being neutron-proton symmetric, and the $^{48}$Ca/$^{64}$Ni + $^{9}$Be reactions with the projectiles both being neutron-rich. The reactions using the relative neutron-proton symmetric projectile was set as the reference reaction denoted by index 1. Theoretically, the relationship between the IBD and isoscaling is described in Eq. (6). The fragment belongs to one isotopic chain and one isotonic chain, thus it can be related to $\alpha$ and $\beta$ according to the respective isotopic and isotonic ratio fitting. For the isobaric chains with $I$ from $-1$ to 2, the IBD and isoscaling results were found to be similar except for some fragments with a large $A$. The IBD results were the same in the $I = 0$ and 1 isobaric chains for the

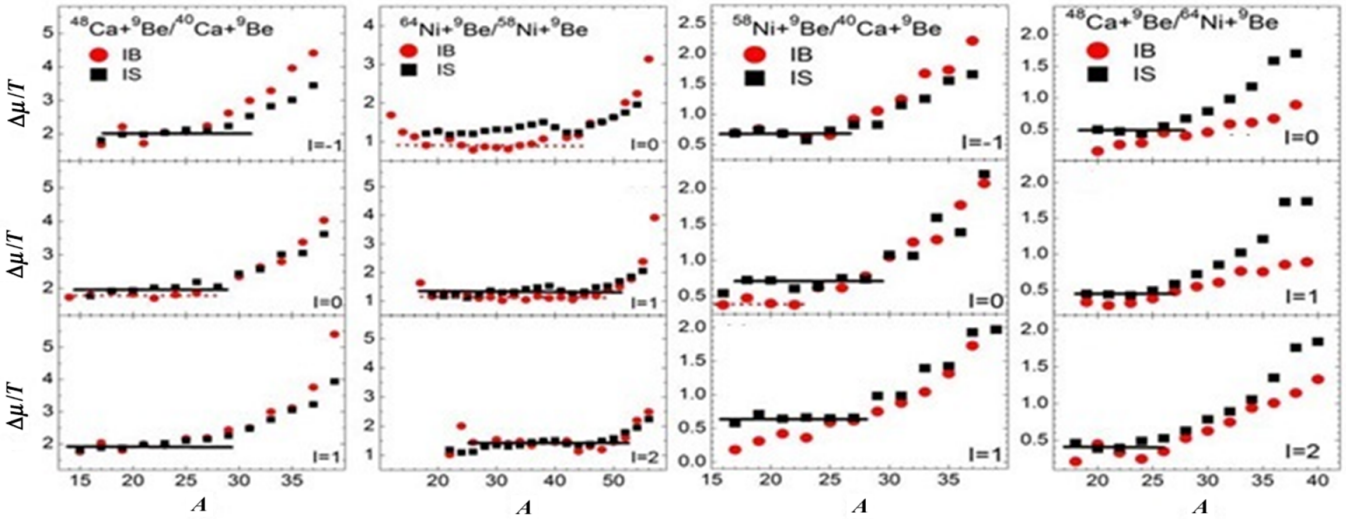


Fig. 1. (Color online) The comparison between the IBD and isoscaling results (a re-plotted figure from Ref. [11]). The circles and squares denote the IBD and isoscaling results, respectively. The lines are just for guiding the eyes to the plateaus in the IBD and isoscaling results.

$^{48}$Ca/$^{40}$Ca reactions. The same phenomena can be found in the $I = 1$ and 2 isobaric chains for the $^{64}$Ni/$^{58}$Ni reactions, and the $I = -1$ isobaric chains for the $^{58}$Ni/$^{40}$Ca reactions.

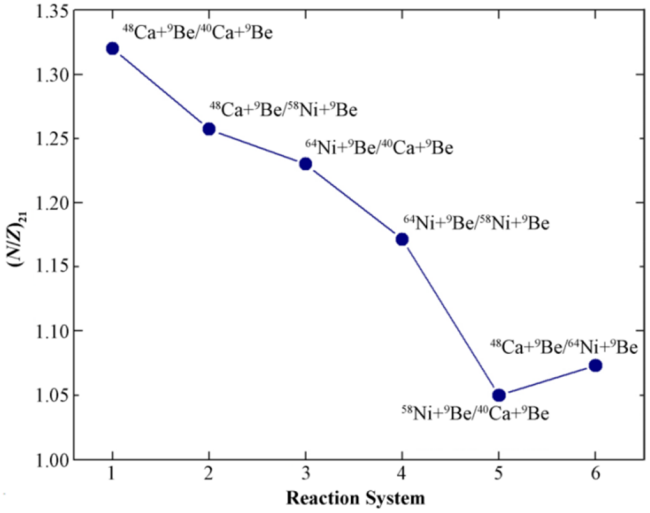


Fig. 2. (Color online) The asymmetry of the systems for obtaining the IBD results. The labels on the circles denote the reactions used.

It was also found that the height of the IBD-plateaus in the four groups were different, about 2, 1.4, 0.5 and 0.4, respectively [11]. And the lengths of the plateaus are also different. In the IBD of neutron-rich isobars, the plateau can disappear [11–14]. The IBD results denote the difference between the neutrons and protons for the two reactions according to Eqs. (9) and (10). If the IBD results change very small, it reflects that the difference between the densities of neutrons and protons for the reactions are small. The increasing IBD with $A$ of the fragment indicates an enlarged difference between the densities of the neutrons and protons [21, 22]. Taking the IBD results for the $^{48}$Ca/$^{40}$Ca reactions as an example, $\rho_{p1}$ and $\rho_{n1}$ for $^{40}$Ca can be assumed to be the same, and assuming that $\rho_{p1} \approx \rho_{p2}$, $\Delta R(I+2, I, A)_{21} = \ln(\rho_{n2}/\rho_{p1})$. $\rho_{n2}$ of the $^{48}$Ca reaction can be determined from the IBD results. For the $^{48}$Ca/$^{40}$Ca reaction, $\Delta R(I+2, I, A)_{21} = \ln(\frac{\rho_{n2}}{\rho_{p1}}) = 2$ which results in $\frac{\rho_{n2}}{\rho_{p1}} = 7.4$. It is very large compared to the isoscaling method. It should be noted that $^{48}$Ca has a much larger neutron excess than $^{40}$Ca, and $\alpha \sim \beta$, of which $\beta$ cannot be omitted in Eq. (6). This makes $\Delta \ln R(I+2, I, A)_{21} = 2\alpha$ , which results in the overestimation of $\frac{\rho_{n2}}{\rho_{p1}}$. Similar explanations can be found for the other three reaction groups. It should be noted that the densities determined by the IBD results are for the time of freeze-out, assuming thermal equilibrium. The relationship between the density of the projectile and the system at the freeze-out should be further studied in transport models.

The IBD-plateau was found to be sensitive to differences between the densities of the reaction systems. The asymmetry of these systems $(N/Z)_{21}$ are calculated and the results are plotted in Fig. 2. The asymmetry of the reaction systems $(N/Z)_{21}$ is defined as $[(N_p+N_t)/(Z_p+Z_t)]_2/[(N_p+N_t)/(Z_p+Z_t)]_1$. From high to low, $(N/Z)_{21}$ is in the order of $^{48}$Ca/$^{40}$Ca, $^{48}$Ca/$^{58}$Ni, $^{64}$Ni/$^{40}$Ca, $^{64}$Ni/$^{58}$Ni, $^{48}$Ca/$^{64}$Ni, and $^{58}$Ni/$^{40}$Ca. The (N/Z)$_{21}$ of the $^{48}$Ca/$^{64}$Ni and $^{58}$Ni/$^{40}$Ca reactions are very similar. In Fig. 3(a), the IBD-results for the $I = 0$ isobaric chain are re-plotted. From high to low, the IBD-plateau is in the order of $^{48}$Ca/$^{40}$Ca, $^{48}$Ca/$^{58}$Ni, $^{64}$Ni/$^{40}$Ca, $^{64}$Ni/$^{58}$Ni, $^{58}$Ni/$^{40}$Ca, and $^{48}$Ca/$^{64}$Ni. The IBD-plateaus for the $^{58}$Ni/$^{40}$Ca and $^{48}$Ca/$^{64}$Ni reactions are very similar. The order of the $(N/Z)_{21}$ and the IBD-plateau are consistent, except for the $^{58}$Ni/$^{40}$Ca and $^{48}$Ca/$^{64}$Ni reactions. The same phenomena can also found in the IBD results for the $I = 1$ isobaric chain in the reactions as plotted in Fig. 3(b).

To test the sensitivity of the IBD-plateau to the density difference between the reactions, we calculate the fragment yield in the $80A$ MeV $^{38\text{-}52}$Ca + $^{12}$C reactions (only the even-

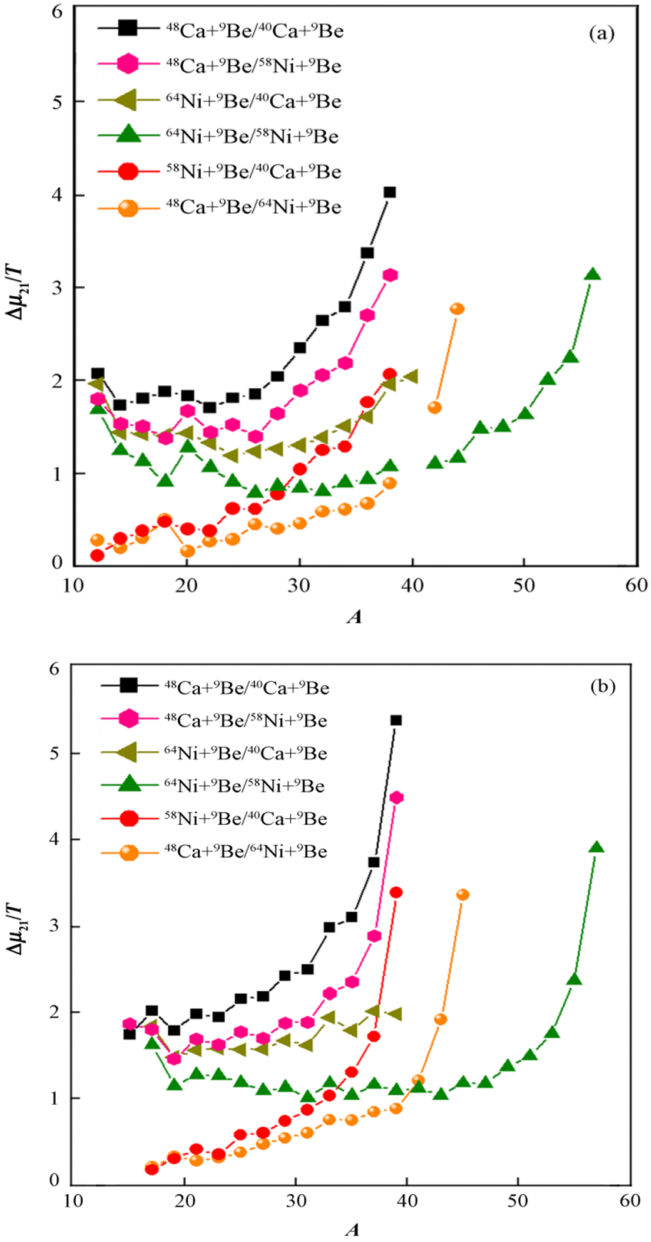


Fig. 3. (Color online) The IBD results for the $I = 0$ (a) and $I = 1$ (b) isobaric chain.

$A$ calcium isotopes are used) by using a modified statistical abrasion-ablation (SAA) model [6, 13, 14, 21–27]. The statistical abrasion-ablation model will not be described in this work. Readers can refer to Refs. [21–27]. The fragments produced in the $^{40}$Ca + $^{12}$C reaction is set as reaction 1, which is the reference reaction. The IBD results for the isobaric chains from $I = -1$ to 2 are plotted in Fig. 4. Since the analyzed fragments are the prefragments which are determined by the neutron and proton densities, as well as the nucleus-nucleus reaction cross sections, the yields of prefragments are sensitive the density changes of the projectile [13]. It is found that, as the projectile ($^{X}$Ca, with $X$ denotes the mass number of projectile) becomes more neutron-rich, the IBD results

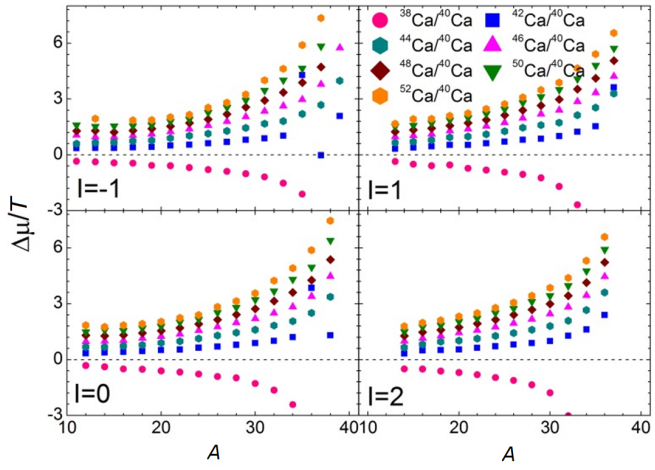


Fig. 4. (Color online) The IBD results for the prefragments calculated by using a modified statistical abrasion-ablation model.

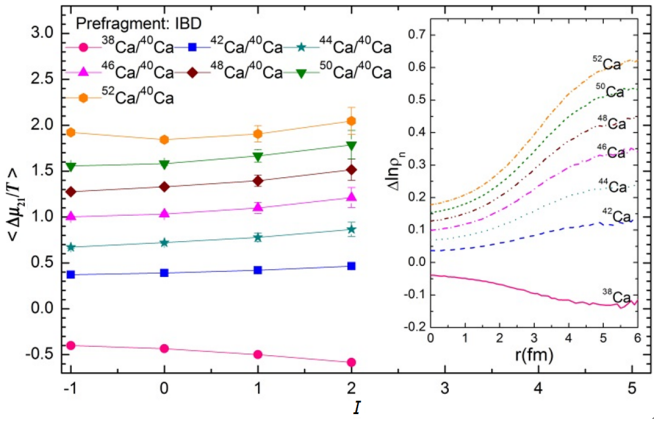


Fig. 5. (Color online) The averaged value of IBD-plateaus for the isobaric chains from $I = -1$ to 2. The inserted figure show the difference between the neutron density distributions of $^{X}$Ca and $^{40}$Ca with $\Delta \ln \rho_n = \ln \rho_n$ ($^{X}$Ca)$- \ln \rho_n$($^{40}$Ca).

increases regularly. The IBD obtained from the prefragments are sensitive to the difference between the neutron density of the $^{X}$Ca and $^{40}$Ca reactions if we assume that the proton densities in $^{X}$Ca are the same or vary very little [13, 14].

We calculated the average values ($< \Delta\mu/T >$) of the IBD-plateau for the isobars plotted in Fig. 4. The $< \Delta\mu/T >$ are plotted as a function of $I$ in Fig. 5. It is shown that for the relative symmetry fragments, $< \Delta\mu/T >$ changes very small with $I$. In the inserted figure of Fig. 5, the difference between the neutron densities ($\Delta \ln \rho_n$) of $^{X}$Ca and $^{40}$Ca is plotted. When $r <\sim 2$ fm, $\Delta \ln \rho_n$ are flat and change very small. It has been illustrated that the yield of fragments with small mass numbers are mostly produced in the central collisions [21, 22, 26, 27]. The flat distribution of $\Delta \ln \rho_n$ between the core part of the calcium isotopes can account for the phenomena of the IBD-plateau. The enlarged $\Delta \ln \rho_n$ with $r$ ($r >\sim 2$ fm for different calcium isotopes) can also account for the increasing of $\Delta\mu$/T with $A$, as well as the disappearance of the

IBD-plateau in the neutron-rich isobars [11–14].

From both the experiment results and the calculated results by the statistical abrasion-ablation model [11–14], it is shown that the IBD probe is sensitive to the density difference between reactions. The IBD probe provides a new method to determine the neutron density in heavy-ion collisions. But as we have noted, the density is for the time of the chemical freeze-out, assuming there is a thermal equilibrium in the reaction. Actually, the process of the reaction is dynamic and changes with reaction time. The IBD results should be verified by a dynamic evolution process. Previously we have reported the IBD result for the $^{58}$Ni + $^{12}$C reaction calculated by the anti-symmetric molecular dynamical (AMD) model to verify the sensitivity of the IBD to density [11]. In dynamical model calculations, the evolution of the IBD results with time can be studied. We have finished the calculations and the IBD analysis of the $^{58,64}$Ni + $^{12}$C reactions and hope to report the AMD results in near future to see the IBD for primary fragments and fragments after the decay process. Moreover, the Shannon information entropy uncertainty is introduced to explain the physical meaning of the IBD probe [28, 29]. In the dynamical model, the construction of fragments are important [30, 31], and at the same time the temperature for heavy fragments should be carefully treated [32–39]. It is also suggested that the IBD can be used to study the evolution of chemical potential and the density of the reactions. We will also study the evolution of the IBD results by using the AMD model.

## IV. SUMMARY

In summary, the method of isobaric yield ratio difference is explained in this work. The IBD method is a more direct method than the isoscaling method to extract the symmetry energy or density of nuclear matter in heavy-ion collisions. It is proven that the IBD probe is sensitive to the difference between the densities of the reactions, and can be used to study the neutron density of the reactions.




[1] Huang M, Chen Z, Kowalski S, *et al*. Isobaric yield ratios and the symmetry energy in heavy-ion reactions near the Fermi energy. Phys Rev C, 2010, **81**: 044620. DOI: 10.1103/PhysRevC.81.044620

[2] Huang M, Bonasera A, Chen Z, *et al*. Isospin dependence of the nuclear equation of state near the critical point. Phys Rev C, 2010, **81**: 044618. DOI: 10.1103/PhysRevC.81.044618

[3] Ma C W, Wang F, Ma Y G, *et al*. Isobaric yield ratios in heavy-ion reactions, and symmetry energy of neutron-rich nuclei at intermediate energies. Phys Rev C, 2011, **83**: 064620. DOI: 10.1103/PhysRevC.83.064620

[4] Ma C W, Pu J, Wei H L, *et al*. Symmetry energy extracted from fragments in relativistic energy heavy-ion collisions induced by $^{124,136}$Xe. Eur Phys J A, 2012, **48**: 78. DOI: 10.1140/epja/i2012-12078-5

[5] Ma C W, Pu J, Wang S S, *et al*. The symmetry energy from the neutron-rich nucleus produced in the intermediate-energy $^{40,48}$Ca and $^{58,64}$Ni Projectile Fragmentation. Chin Phys Lett, 2012, **29**: 062101. DOI: 10.1088/0256-307X/29/6/062101

[6] Ma C W, Song H L, Pu J, *et al*. Symmetry energy from neutron-rich fragments in heavy-ion collisions, and its dependence on incident energy, and impact parameters. Chin Phys C, 2013, **37**: 024102. DOI: 10.1088/1674-1137/37/2/024102

[7] Marini P, Bonasera A, Mclntosh A, *et al*. Constraining the symmetry term in the nuclear equation of state at subsaturation densities and finite temperatures. Phys Rev C, 2012, **85**: 034617. DOI: 10.1103/PhysRevC.85.034617

[8] Marini P, Bonasera A, Souliotis G A, *et al*. Systematic study of the symmetry energy within the approach of the statistical multifragmentation model. Phys Rev C, 2013, **87**: 024603. DOI: 10.1103/PhysRevC.87.024603

[9] Mallik S and Chaudhuri G. Symmetry energy from nuclear multifragmentation. Phys Rev C, 2013, **87**: 011602. DOI: 10.1103/PhysRevC.87.011602

[10] Mallik S and Chaudhuri G. Effect of particle fluctuation on isoscaling and isobaric yield ratio of nuclear multifragmentation. Phys Lett B, 2013, **727**: 282–286. DOI: 10.1016/j.physletb.2013.10.011

[11] Ma C W, Wang S S, Zhang Y L, *et al*. Isobaric yield ratio difference in heavy-ion collisions, and comparison to isoscaling. Phys Rev C, 2013, **87**: 034618. DOI: 10.1103/PhysRevC.87.034618

[12] Ma C W, Wang S S, Zhang Y L, *et al*. Chemical properties of colliding sources in $^{124,136}$Xe and $^{112,124}$Sn induced collisions in isobaric yield ratio difference and isoscaling methods. J Phys G Nucl Partic, 2013, **40**: 125106. DOI: 10.1088/0954-3899/40/12/125106

[13] Ma C W, Yu J, Bai X M, *et al*. Isobaric yield ratio difference and neutron density difference in calcium isotopes. Phys Rev C, 2014, **89**: 057602. DOI: 10.1103/PhysRevC.89.057602

[14] Ma C W, Bao X M, Yu J, *et al*. Neutron density distributions of neutron-rich nuclei studied with the isobaric yield ratio difference. Eur Phys J A, 2014, **50**: 139. DOI: 10.1140/epja/i2014-14139-1

[15] Das C B, Gupta S D, Liu X D, *et al*. Comparison of canonical and grand canonical models for selected multifragmentation data. Phys Rev C, 2001, **64**: 044608. DOI: 10.1103/PhysRevC.64.044608

[16] Tsang M B, Lynch W G, Friedman W A, *et al*. Fragmentation cross sections and binding energies of neutron-rich nuclei. Phys Rev C, 2007, **76**: 041302(R). DOI: 10.1103/PhysRevC.76.041302

[17] Xu H S, Tsang M B, Liu T X, *et al*. Isospin fractionation in nuclear multifragmentation. Phys Rev Lett, 2000, **85**: 716. DOI: 10.1103/PhysRevLett.85.716

[18] Tsang M B, Friedman, Gelbke C K, *et al*. Isotopic scaling in nuclear reactions. Phys Rev Lett, 2001, **86**: 5023. DOI: 10.1103/PhysRevLett.86.5023

[19] Geraci E, Bruno M, D'Agostino M, *et al*. Isoscaling in central $^{124}$Sn+$^{64}$Ni, $^{112}$Sn+$^{58}$Ni collisions at 35$A$ MeV. Nucl Phys A, 2004, **732**: 173–201. DOI: 10.1016/j.nuclphysa.2003.11.055

[20] Mocko M, Tsang M B, Andronenko L, *et al*. Projectile fragmentation of $^{40}$Ca, $^{48}$Ca, $^{58}$Ni, and $^{64}$Ni at 140 MeV/nucleon. Phys Rev C, 2006, **74**: 054612. DOI: 10.1103/PhysRevC.74.054612

[21] Ma C W, Wang S S, Wei H L, *et al*. Re-examination of finite-size effects in isobaric yield ratios using a statistical Abrasion-

Ablation model. Chin Phys Lett, 2013, **30**: 052101. DOI: 10.1088/0256-307X/30/5/052501

[22] Ma C W, Wei H L and Ma Y G. Neutron-skin effects in isobaric yield ratios for mirror nuclei in a statistical abrasion-ablation model. Phys Rev C, 2013, **88**, 044612. DOI: 10.1103/PhysRevC.88.044612

[23] Gaimard J J and Schmidt S H. A reexamination of the abrasion-ablation model for the description of the nuclear fragmentation reaction. Nucl Phys A, 1991, **531**: 709–745. DOI: 10.1016/0375-9474(91)90748-U

[24] Brohm T and Schmidt K H. Statistical abrasion of nucleons from realistic nuclear-matter distributions. Nucl Phys A, 1994, **569**: 821–832. DOI: 10.1016/0375-9474(94)90386-7

[25] Fang D Q, Shen W Q, Feng J, *et al*. Isospin effect of fragmentation reactions induced by intermediate energy heavy ions and its disappearance. Phys Rev C, 2000, **61**: 044610. DOI: 10.1103/PhysRevC.61.044610

[26] Ma C W, Wei H L, Wang J Y, *et al*. Isospin dependence of projectile-like fragment production at intermediate energies. Phys Rev C, 2009, **79**: 034606. DOI: 10.1103/PhysRevC.79.034606

[27] Ma C W, Wei H L, Liu G J, *et al*. Systematic behavior in the isospin dependence of projectile fragmentation of mirror nuclei with $A = 20$–$60$. J Phys G Nucl Partic, 2010, **37**: 015104. DOI: 10.1088/0954-3899/37/1/015104

[28] Ma C W and Wei H L. Isotopic ratio, isotonic ratio, isobaric ratio and Shannon information uncertainty. Commun Theor Phys, 2014, **62**: 717–720.

[29] Ma C W, Wei H L, Wang S S, *et al*. Isobaric yield ratio difference and Shannon information entropy. Phys Lett B, 2015, **742**: 19–22. DOI: 10.1016/j.physletb.2015.01.015

[30] Lin W, Wada R, Huang M, *et al*. Experimental reconstruction of primary fragments with kinematical focusing method. Nucl Sci Tech, 2013, **24**: 050511.

[31] Wada R, Hang M, Lin W, *et al*. IMF production and symmetry energy in heavy ion collisions near Fermi energy. Nucl Sci Tech, 2013, **24**: 050501.

[32] Ma C, Qiao C, Wang S, *et al*. Temperature and symmetry energy of neutron-rich fragments in the 1A GeV $^{124,136}$Xe+Pb reactions. Nucl Sci Tech, 2013, **24**: 050510.

[33] Su J and Zhang F S. Isotopic dependence of nuclear temperatures. Phys Rev C, 2011, **84**: 037601. DOI: 10.1103/PhysRevC.84.037601

[34] Su J, Zhu L, Xie W J, *et al*. Nuclear temperatures from kinetic characteristics. Phys Rev C, 2012, **85**: 017604. DOI: 10.1103/PhysRevC.85.017604

[35] Ma C W, Pu J, Ma Y G, *et al*. Temperature determined by isobaric yield ratios in heavy-ion collisions. Phys Rev C, 2012, **86**: 054611. DOI: 10.1103/PhysRevC.86.054611

[36] Ma C W, Zhao X L, Pu J, *et al*. Temperature determined by isobaric yield ratios in a grand-canonical ensemble theory. Phys Rev C, 2013, **88**: 014609. DOI: 10.1103/PhysRevC.88.014609

[37] Ma C W, Wang S S, Pu J, *et al*. Temperature of heavy fragments in heavy-ion collisions. Commun Theor Phys, 2013, **59**: 95–98.

[38] Wu H Y, Xiao Z G, Jin G M, *et al*. Evidence of "slow" relaxation of isospin degree of freedom. Phys Lett B, 2002, **538**: 39–44. DOI: 10.1016/S0370-2693(02)01971-8

[39] Ma C W, Zhang Y L, Qiao C Y, *et al*. Target effects in isobaric yield ratio differences between projectile fragmentation reactions. Phys Rev C, 2015, **91**: 014615. DOI: 10.1103/PhysRevC.91.014615